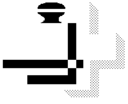

Eidgenössisches Amt für Messwesen
Office fédéral de métrologie
Ufficio federale di metrologia
Swiss Federal Office of Metrology

WGDM-7: Preliminary comparison on nanometrology
According to the rules of CCL key comparisons

Nano4: 1D gratings

Final report

Draft B

Wabern, 30. November 2000 / F. Meli

Blank

Content

1. Introduction 4

2. Organisation 4
2.1 Participants 4
2.2 Time schedule 6

3. Standards 7
3.1 Description 7
3.3 Sample mounting 7
3.4 Handling and damages 7

4. Measurand 8

5. Methods of measurement 8

6. The Stability of the standards 9

7. Comparison of the two sets of gratings 10

8. Measurement results 11

9. Analysis 14

10. Uncertainty budgets 16

11. Discussions, conclusions and remarks 17

Appendix A: A1
Description of the measurement methods and instruments by the participants

1. Introduction

The metrological equivalence of national measurement standards is determined by a set of key comparisons chosen and organised by the Consultative Committees of the CIPM or by the Regional Metrology Organisations (ROM's) in collaboration with the Consultative Committees.
At its meeting in September 1997, the Consultative Committee for Length, CCL, identified several key comparisons in the field of dimensional metrology and decided upon the general content. As the field of Nanometrology is one of the most recent fields in Dimensional Metrology the particular key comparisons were not yet fixed.
Therefore the discussion group for nanometrology (WGDM-7 DG) has decided at the June 98 meeting at BIPM, to perform preliminary comparisons on the following five topics:

Nano1 Line width standards
Nano2 Step height standards
Nano3 Line scales
Nano4 1D gratings
Nano5 2D gratings

In particular, the DG has decided that a comparison with 1D gratings should start by the end of 1998, with the Swiss Federal Office of Metrology (OFMET) as the pilot laboratory.
As the rules for key comparisons were followed it may be declared as such in future or, at least, be recognised as a comparison used to establish metrological equivalence and thus be included in the MRA App. B data base.

2. Organisation

Following the rules set up by the BIPM[1] a small group from the provisional list of participating laboratories has drafted the technical protocol in 1998. The group was composed of the pilot laboratory (Felix Meli from OFMET, Switzerland), Leonid Vitushkin from the BIPM, France and Joergen Garnaes from DFM, Denmark.
The comparison started in February 1999 with the circulation of the standards among the 12 participants within two loops.

2.1 Participants

The list of participants for this comparison includes everybody attending the WGDM7 DG meeting in June 98 at the BIPM who was willing to participate in the Nano4 comparison. Additionally, VNIIM, NRLM and KRISS agreed also to participate. In this way the different metrology regions were adequately represented.

[1] T.J. Quinn, Guidelines for key comparisons carried out by Consultative Committees, draft of 15. May 1998, BIPM, Paris.

Table 1: List of Participants

Leonid Vitushkin	BIPM Pavillon de Breteuil 92312 Sèvres Cedex France	Tel. +33 1 45 07 7075 Fax +33 1 45 07 7049 e-mail: lvitushkin@bipm.fr
Gwo-Sheng Peng	CMS/ITRI Bldg. 16 321 Kuang Fu Rd, Sec. 2 Hsinchu Taiwan 300	Tel. +886 3 573 2150 Fax +886 3 572 6445 e-mail: 810603@cms.itri.org.tw
Joergen Garnaes and Niels Kofod	DFM Building 307 Anker Engelunds Vej 1 DK-2800 Lyngby Denmark	Tel. +45 45 25 5884 Fax +45 45 93 1137 e-mail: jg@dfm.dtu.dk
Marco Pisani	IMGC Strada delle Cacce 73 10135 Torino Italy	Tel. +39 011 39 771 Fax +39 011 39 77 459 e-mail: pisani@imgc.to.cnr.it
Byong Chon Park	KRISS P.O.Box 102 Yusong Taejon 305-600 Korea	Tel. +82 42 868 5209 Fax +08 42 868 5012 e-mail: kyu@kriss.re.kr
Xu Yi and Gao Sitian	NIM No. 18, Bei San Huan Dong Lu Beijing 100013 China	Tel. +86 Fax +86 10 6421 8703 e-mail: xuyi@public.bta.net.cn
Theodore Vorburger and Ronald Dixon	NIST Room A117, Metrology Building Gaithersburg, MD 20899-0001 USA	Tel. +1 301 975 3493 Fax +1 301 869 0822 e-mail: theodore.vorburger@nist.gov
Keith Jackson	NPL Centre for Basic, Thermal and Length Metrology Teddington Middlesex TW11 OLW England	Tel. +44 208 977 3222 Fax +44 208 943 2945 e-mail: keith.jackson@npl.co.uk
Tomizo Kurosawa	NRLM Mechanical Metrology Department 1-1-4 tsukuba Ibaraki 305-8563 Japan	Tel. +81 298 61 4041 Fax +81 298 61 4042 e-mail: kurosawa@nrlm.go.jp
Günter Wilkening and Werner Mirandé	PTB Gruppe 5.1 Postfach 3345 D-38023 Braunschweig Germany	Tel. +49 531 592 5100 Fax. +49 531 592 9292 e-mail: guenter.wilkening@ptb.de
Alexander Korolev	VNIIM 19, Perspective de Moskovsky 198005 St. Petersburg Russia	Tel. +7 812 251 8638 Fax + 812 113 0114 e-mail: post@length.vniim.spb.su

Coordinator:		
Felix Meli	OFMET Swiss Federal Office of Metrology Lindenweg 50 CH-3003 Bern-Wabern Switzerland	Tel. +41 31 323 3346 Fax +41 31 323 3210 e-mail: felix.meli@eam.admin.ch

2.2 Time schedule

The comparison started in February 1999 with the initial measurements at OFMET. Due to the large number of participating laboratories, the time schedule was tight and only one month had been foreseen for each laboratory for the calibration including the transportation. To catch up some lost time in the first loop the comparison was made finally in two loops instead of the planned three.
As the gratings were severely damaged when they came back to the pilot laboratory the first time, the gratings had to be replaced by a set of new gratings.
The following table shows the scheduled measuring time, the date of reception of the standards and the date when the results were received by the pilot laboratory. Dates in parenthesis are estimates as no confirmation of reception was received.

Table 2: Time schedule

Laboratory	Original schedule	Confirmation of reception	Results received
1st loop with first set of gratings:			
OFMET	February 1999	-	20.2.1999
DFM	March 1999	(8.3.1999)	26.6.2000
PTB	April 1999	1.4.1999	5.1.2000
BIPM	May 1999	10.5.1999	None*
IMGC	June 1999	(11.6.1999)	23.9.1999
OFMET	August 1999	21.7.1999	17.8.1999
2nd loop with second set of gratings:			
OFMET	August 1999	1.8.1999	20.8.1999
NIST	September 1999	27.8.1999	2.6.2000
NPL	October 1999	1.10.1999	15.12.1999
VNIIM	November 1999	19.11.1999	28.1.2000
OFMET	December 1999	By-passed	-
NIM	January 2000	20.1.2000	16.6.2000
NRLM	February 2000	11.2.2000	30.6.2000
CMS	March 2000	20.3.2000	30.5.2000
KRISS	April 2000	27.4.2000	29.6.2000
OFMET	May 2000	2.6.2000	20.6.2000

* The BIPM method (see also VNIIM) requires large gratings with a very good flatness. Apparently the used standards did no satisfy this condition and therefore no measurement results were obtained.

3. Standards

At the WGDM7 DG meeting in June 98 at the BIPM, it was decided to use 1D gratings with pitches between 200nm and 1000nm in accordance with the agreed definition of nanometrology. The standards should meet the requirements of different measuring methods such as SEM, STM, AFM or laser diffraction leaving the participants the flexibility to choose their preferred method.

3.1 Description

Two holographic gratings with pitches of nominally 700nm and 290nm were chosen. These SEM calibration gratings manufactured by Moxtek (MXS 301CE and MXS 701CE, (http://www.moxtek.com/standards/semcl1ds.htm) are on a piece of silicon with the size of 4mm x 3mm x 0.5mm. The holographic grating is recorded into a polymer resist material on the silicon surface and is coated with a 60nm tungsten film. The ribs with heights of about 200nm have a somewhat rounded rather than completely flat top surface. The edges of the ribs exhibit an edge location variation which is less than 10nm. The mostly clean and uniform pattern on the standards has a few imperfections which can be used as focusing aids.

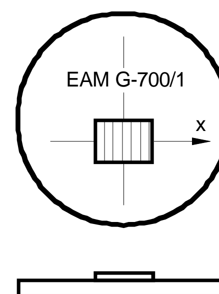

Fig. 1: Standard on steel disk

3.3 Sample mounting

The standards were mounted with conductive carbon tabs onto steel disks ∅ 15mm and thickness 2mm (Fig. 1). Engraved on the steel disk is the identification and the measurement direction (→ x). This mounting is intended for magnetic holding as used in most SPM's. Additionally each standard comes with an aluminium base plate 30mm x 30mm which incorporates a magnet (Fig. 2). The standard could be clamped onto this plate for mechanical holding in diffractometers and other equipment. The height from the base plate bottom to the grating surface is 10mm.

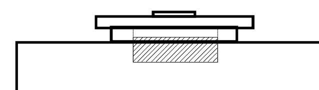

Fig. 2: Standard on base plate with magnet

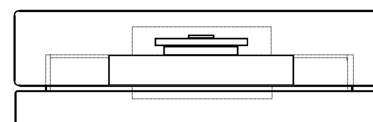

Fig. 3: Complete assembly in container

3.4 Handling and damages

The participants were asked to handle the standards carefully, to keep them clean and to take care that no damage of the standards occurs. Nevertheless, when the gratings came back from the first loop they were severely damaged probably by a stylus profiler and by scratches. At that time it was decided to replace the gratings by a new set. The second set survived the full second loop although also here several scratches were found at the end. On the last transportation to OFMET two corners of the 300nm standard broke off. The damage in the central measuring area of the second set of standards remained acceptable. The identification of the gratings from the first set (referred to as set 1) were G-300/1 and G-700/1 and for the second set (set 2) G-300/3 and G-700/3.

4. Measurand

The measurand used in this comparison **was the average pitch over a surface of 1mm x 1mm in the centre of the standard at 20°C. The direction of the pitch is defined to be orthogonal to the ribs of the grating.** This direction is not necessarily parallel to the long side of the chip or to the arrow marking the x-direction.
A complete description of the applied method and a detailed estimation of the measurement uncertainty according to the *ISO Guide to the Expression of Uncertainty in Measurement (GUM)* was asked for.

5. Methods of measurement

The participants were free to choose the method of measurement. They could even supply more than one measurement result if independent measuring techniques were applied. NPL and OFMET have supplied results for two methods while all others used one method.
Besides the very successful optical diffraction technique (OD), an optical microscope (OM) and scanning probe instruments SPM (AFM = atomic force microscope) were used.
The full description of the measurement methods and instruments by the participants can be found in the appendix A. The following table gives a brief overview:

Table 3: Methods of measurement

Laboratory	Principle	Instruments and traceability
DFM	SPM	Commercial AFM with capacitive position sensors (DI metrology head). Calibration of AFM head with an IBSEN grating traceable to NPL. A special calibration software was used (SPIP). Image size typ. 50 µm x 6.5 µm
PTB	OD	Good Littrow diffraction approximation, Ar-laser with three wavelengths (W.R. Benett, Atomic gas laser transition data, IFI/Plenum), precision angle encoder (Heidenhain RON 255), CMOS array detector at 4 m distance.
IMGC	OD	Littrow diffraction, red and green He-Ne laser, goniometric table, two quadrant photo-detector.
NIST	SPM	NIST C-AFM with heterodyne laser interferometer (laser NIST traceable), closed loop control of the lateral sample position. Image size 1.5 - 3.5 µm.
NPL1	OD	Littrow diffraction, green He-Ne laser, manual angle table with two reading heads, optical screen.
NPL2	OM	Optical microscope, linear translation stage with laser interferometer (laser NPL traceable). For 700 nm grating only.

VNIIM	OD	Laser interference diffractometer with reference line scale (comparator). Line scale (5µm) traceable to VNIIM. Argon Laser with two wavelengths (R.J. Pressley (Ed.), Handbook of lasers, Chemical Rubber Co, Cleveland, 1971).
NIM	OD	Littrow diffraction based, green He-Ne laser, precision angle encoder (inductosyn), two quadrant photo-detector.
NRLM	SPM	NRLM AFM with three-axis laser interferometer (laser NRLM traceable), line scans of 10 - 17.5 µm and 5500 - 8000 data-points.
CMS	SPM	Commercial AFM with capacitive position sensors (DI metrology head). Calibration of AFM head with Moxtek grating and factory certificate. Image analysis with SPIP software. Image size 3 µm and 7 µm
KRISS	OD	Littrow diffraction, Argon laser at 487.986 nm (Handbook of Laser Wavelengths, CRC, 1999, p. 308), calibrated angle encoder (Heidenhain ERO 725), four quadrant photo-detector.
OFMET1	OD	Littrow diffraction, red and green He-Ne laser (OFMET traceable), rotary table with air bearings, friction wheel drive and piezo fine adjustment, calibrated precision angle encoder (Heidenhain RON 905), four quadrant photo-detector.
OFMET2	SPM	OFMET AFM profiler with interferometric long range linear displacement stage (laser OFMET traceable). Linescans 288 µm and 350 µm, local ridge detection based on 1000 points per pitch. AFM with DI metrology head.

6. The Stability of the standards

The standards were exposed to considerable temperature variations during the transportation. The temperature varied at least between -11°C and 32°C (Fig. 4).

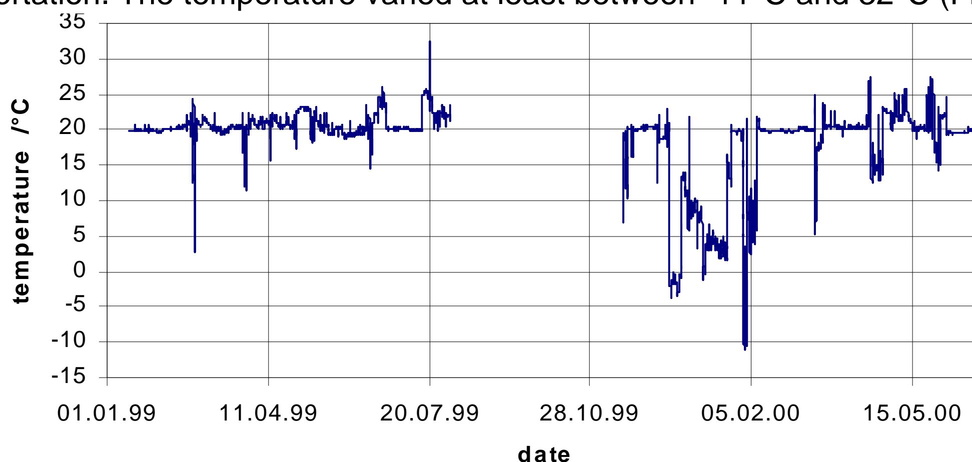

Fig. 4: Temperature measurements of the data logger during the journey of the gratings. The temperature varied at least between -11°C and 32°C. As the second stop at OFMET was omitted some values are missing.

To ensure that the standards remained stable over these 18 months, control measurements were performed at OFMET before and after the comparison for each of the two sets of gratings, see table 4. The difference of the diffraction measurements were well below the measurement uncertainty and it is therefore concluded that **the standards were stable** during the time of the comparison.

Table 4: Pitch difference final-initial and its combined standard uncertainty measured at OFMET with optical diffraction.

Grating:	G-300	G-700
/1 (set1)	(0.003±0.005) nm	(0.000±0.014) nm
/3 (set2)	(0.000±0.005) nm	(0.003±0.007) nm

The participants were asked to inspect the gratings for damages on the measurement surface. The quality of the gratings decreased continuously during the comparison. However, the central measurement area of 1mm x 1mm remained almost unchanged. Only the G-700/1 grating was severely damaged after the first loop. Nevertheless also in this case the standard could still be measured at OFMET by laser diffraction although with a slightly increased uncertainty.

7. Comparison of the two sets of gratings

Due to the already mentioned damage, the first set of gratings was replaced after the first loop by a second set. The Moxtek serial numbers of the gratings were quite close to each other indicating that the two sets were probably processed in the same batch. The two sets of gratings were compared to each other at OFMET (Fig. 5 and 6).

From all the measurements made at OFMET, i.e. OD initial and final and the AFM measurements at the beginning, weighted mean values for the pitch of the gratings of set1 and set2 were calculated:

Table 5: OFMET reference pitches and their combined standard uncertainty for set1 and set2 obtained from all measurements made with optical diffraction and AFM profiler at OFMET.

Grating:	G-300	G-700
/1 (set1)	(287.5987±0.0023) nm	(700.7628±0.0039) nm
/3 (set2)	(287.5983±0.0024) nm	(700.7699±0.0033) nm
combined 1&2	(287.5985±0.0016) nm	(700.7669 ±0.0025) nm
difference 2-1	(0.000±0.003) nm	(0.007±0.005) nm

The pitch difference between the two G-300 gratings is well below one standard uncertainty and for the G-700 gratings it is 1.4 standard uncertainties.

It is therefore assumed that the corresponding gratings of **the two sets are identical**. This will allow an easy comparison of all measurements made by the different laboratories without taking into account any pitch difference.

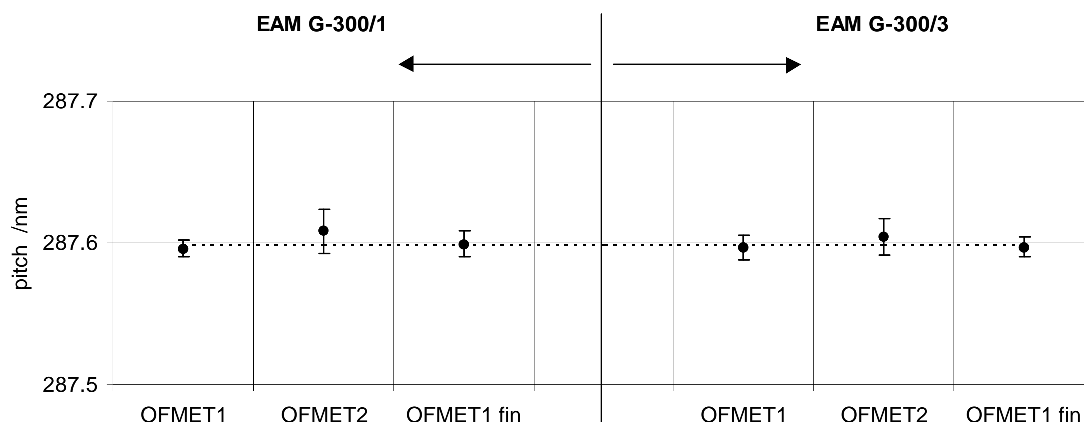

Fig. 5: OFMET measurements on the G-300 gratings. OFMET1 indicates diffraction measurements performed at the beginning and OFMET1fin at the end of the comparison. OFMET2 indicates AFM profiler measurements performed at the beginning of the comparison. The error bars show the measurement uncertainty at a confidence level of 95%. The dotted line represents the weighted mean of all values.

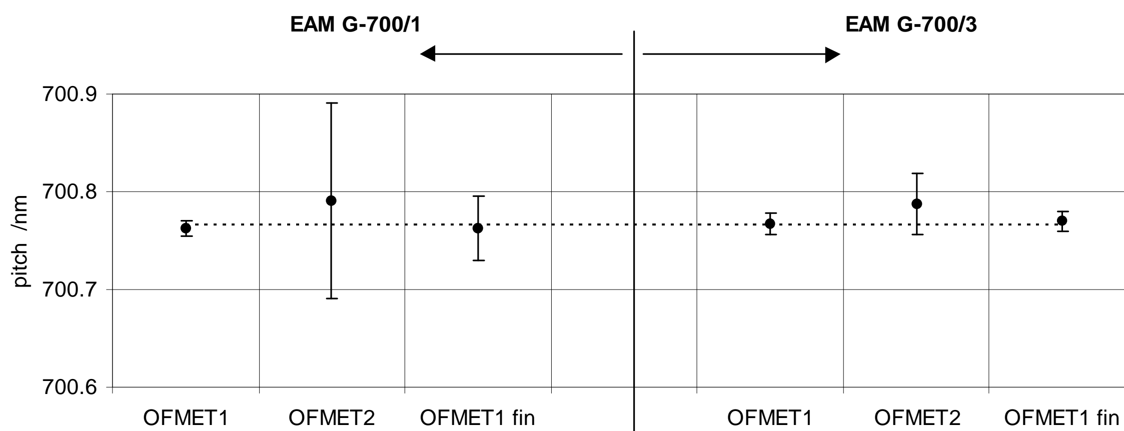

Fig. 6: OFMET measurements on the G-700 gratings. OFMET1 indicates diffraction measurements performed at the beginning and OFMET1fin at the end of the comparison. OFMET2 indicates AFM profiler measurements performed at the beginning of the comparison. The error bars show the measurement uncertainty at a confidence level of 95%. The dotted line represents the weighted mean

8. Measurement results

In the following the results received from the participants are presented. Table 6 and figure 7 show the results for the G-300 gratings while table 7 and figure 8 show those for the G-700 gratings. Besides the measured value for the pitch p, the combined standard uncertainty u_c and the degree of freedom n_{eff} is listed. n_{eff} -values of infinity submitted by the participants were replaced by a value of 1000 for the subsequent calculations.

For the final report (Draft B) VNIIM has submitted a new higher uncertainty value for the G-700 grating explained by an error in a sensitivity coefficient. Now u_c = 0.86 nm (Draft A: 0.5 nm) and ν_{eff} = 867 (86). This change had no effect on the reference value. The En value for this measurement lowered to 0.63 (before 1.07).

Table 6: Measurement results for the G-300 gratings. Pitch p, the combined standard uncertainty u_c and the degree of freedom ν_{eff}.

	p (nm)	u_c (nm)	ν_{eff}
First loop: G-300/1			
OFMET 1	287.5962	0.0029	20.8
OFMET2	287.608	0.006	5.6
DFM	287.47	0.20	∞
PTB	287.5923	0.0032	∞
IMGC	287.600	0.005	106
Second loop: G-300/3			
OFMET1	287.5972	0.0041	19
OFMET2	287.604	0.006	12.7
NIST	287.01	0.36	68.8
NPL 1	287.597	0.004	∞
VNIIM	287.4	0.2	39
NIM	287.5950	0.0015	47
NRLM	287.586	0.074	19
CMS	287.4	0.99	12
KRISS	287.5899	0.0020	89

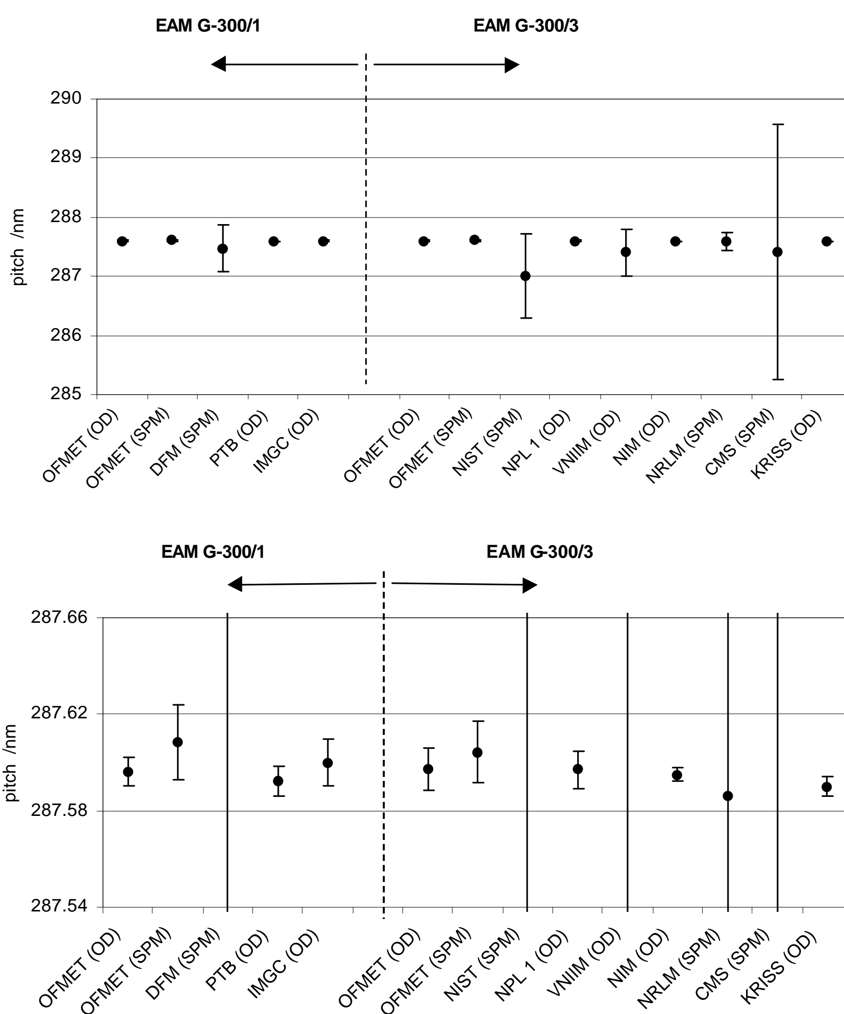

Fig. 7: Measurement results for the G-300 gratings. The error bars show the expanded measurement uncertainty at a confidence level of 95%. Top: full range, bottom with expanded y-scale.

Table 7: Measurement results for the G-700 gratings. Pitch p, the combined standard uncertainty u_c and the degree of freedom n_{eff}.

	p (nm)	**u_c (nm)**	**n_{eff}**
First loop: G-700/1			
OFMET 1	700.7624	0.0041	28.9
OFMET2	700.790	0.039	5.4
DFM	700.38	0.48	∞
PTB	700.7956	0.0078	∞
IMGC	700.754	0.048	78
Second loop: G-700/3			
OFMET1	700.7673	0.0050	19
OFMET2	700.788	0.013	7.0
NIST	700.1	1.0	35.2
NPL 1	700.765	0.022	∞
NPL 2	700.80	0.15	500
VNIIM	699.7	0.86	867
NIM	700.768	0.019	53
NRLM	700.814	0.220	8
CMS	698.1	2.4	12
KRISS	700.7534	0.0036	486

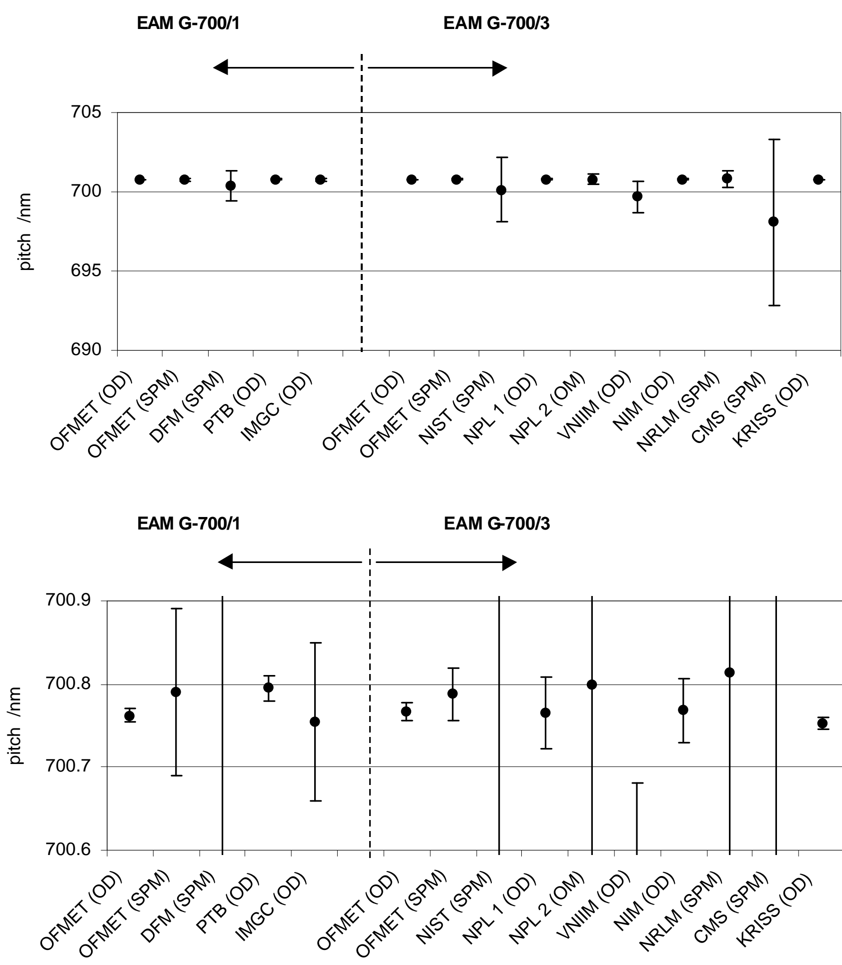

Fig. 8: Measurement results for the G-700 gratings. The error bars show the expanded measurement uncertainty at a confidence level of 95%. Top: full range, bottom with expanded y-scale.

9. Analysis

Reference value:
As already mentioned in the instructions, the reference value (x_{ref}) for this comparison is calculated as the weighted mean of all measurements (x_i). The weights are $u^{-2}(x_i)$. Due to the very different methods applied by the different laboratories the uncertainties vary by a factor of 660. In this situation an unweighted mean is not useful.
As the measurements at OFMET revealed no clear difference between the two sets of gratings it is assumed that the corresponding gratings of the two sets are identical. Therefore, for each type of grating only one reference value was calculated. The OFMET measurements on both sets of gratings were used in the comparison, however always only the initial ones made on each set.

With the given combined uncertainties $u^{-2}(x_i)$ and their effective degrees of freedom $\nu_{eff}(x_i)$ the $En(x_i)$ values with a confidence value of 95% were determined. Measurements with En_{95} values larger than one were omitted one by one for the calculation of the reference value. Finally all values contributing to the reference value had En_{95} values ≤ 1.

$$x_{ref} = \frac{\sum_{i=1}^{n} u^{-2}(x_i) \cdot x_i}{\sum_{i=1}^{n} u^{-2}(x_i)} \tag{1}$$

$$u_c(x_{ref}) = \left(\sum_{i=1}^{n} u^{-2}(x_i) \right)^{-1/2} \tag{2}$$

$$\nu_{eff}(x_{ref}) = \frac{u_c^{\,4}(x_{ref})}{\sum_{i=1}^{n} \frac{u_i^{\,4}(x_{ref})}{\nu_{eff}(x_i)}} \quad \text{with} \quad u_i(x_{ref}) = |c_i| \cdot u(x_i) = \frac{u^{-2}(x_i)}{\sum_{i=1}^{n} u^{-2}(x_i)} \cdot u(x_i) \tag{3}$$

$$U_{95}(x_{ref}) = u_c(x_{ref}) \cdot k_{95} \quad \text{with} \quad k_{95} = t_{95}(\nu_{eff}(x_{ref})) \tag{4}$$

$$En_{95}(x_i) = \left| \frac{x_i - x_{ref}}{\sqrt{U_{95}^{\,2}(x_i) + U_{95}^{\,2}(x_{ref})}} \right| \tag{5}$$

The plus sign in the denominator of (5) is used here although there is some correlation between a single measurement result and the reference value. This correlation depends on the weight this single measurement has with respect to others. With the plus sign used here for simplicity, the *En* values could be slightly too small which is in favour of laboratories with *En* values near 1.

For the calculation of the comparison reference values only 2 of the totally 29 measurements had to be omitted. The corresponding *En* values before the exclusion were: 2.0 for G-700 PTB and 1.1 for G-300 KRISS. For the results finally included in the calculation of the reference value the average *En* values were 0.36 and 0.40 for the G-300 and the G-700 gratings.

Table 8: The comparison Reference value p_{ref} the combined standard uncertainty u_c, the resulting degree of freedom n_{eff} and the expanded uncertainty U_{95} obtained from all measurements with En £ 1.

Gratings:	G-300	G-700
p_{ref}	287.5961 nm	700.7607 nm
u_c	0.0011 nm	0.0023 nm
n_{eff}	146	159
U_{95}	0.0021 nm	0.0046 nm

Table 9: Deviations dp and En values for the G-300 and G-700 gratings. Shaded results have En values > 1

Gratings:	G-300		G-700	
	dp **(nm)**	***En***	***dp*** **(nm)**	***En***
First loop:				
OFMET 1	0.0001	0.01	0.0017	0.18
OFMET2	0.0123	0.78	0.0297	0.30
DFM	-0.1261	0.32	-0.3807	0.40
PTB	-0.0038	0.57	0.0349	2.18
IMGC	0.0039	0.39	-0.0067	0.07
Second loop:				
OFMET1	0.0011	0.13	0.0066	0.58
OFMET2	0.0081	0.63	0.0272	0.85
NIST	-0.5861	0.82	-0.6607	0.33
NPL 1	0.0009	0.11	0.0043	0.10
NPL 2			0.0393	0.13
VNIIM	-0.1961	0.48	-1.0607	0.63
NIM	-0.0011	0.29	0.0073	0.19
NRLM	-0.0101	0.07	0.0533	0.11
CMS	-0.1961	0.09	-2.6607	0.51
KRISS	-0.0062	1.37	-0.0073	0.87

Birge ratio:

The Birge ratio is calculated to check the consistency of the estimated uncertainties with the variation of the different results. The Birge ratio is defined as:

$$R_B = \frac{s_{ext}}{s_{\text{int}}} \quad \text{with} \quad s_{ext} = \sqrt{\frac{\sum_i \left((x_i - x_{ref}) / u_i \right)^2}{(n-1) \cdot \sum_i u_i^{-2}}} \quad \text{and} \quad s_{\text{int}} = u_c(x_{ref}) \qquad (6)$$

where s_{ext} expresses a weighted standard deviation of the results x_i.

If all results are used to calculate R_B (including those with $En > 1$), R_B is 1.25 for the G-300 gratings and 1.54 for the G-700 gratings.
Subsequently only results with $En \leq 1$ were used to calculate R_B. For the G-300 gratings R_B is then 1.03 while for the G-700 gratings R_B is 1.17. For the small number of measurements (n=14 or 15) the reported results and their associated uncertainties can be considered consistent.

10. Uncertainty budgets

The participants were asked to deliver an uncertainty estimation according to the *ISO Guide to the Expression of Uncertainty in Measurement (GUM)*. In order to achieve a better comparability some possible influence parameters were already mentioned in the instructions. The participating laboratories were encouraged to use all known influence parameters for their applied method. Therefore the uncertainty budgets were as different as the measurement methods. Also for similar methods the budgets were structured quite differently.

Most laboratories included the following contributions in the uncertainty budget (method dependent):

- Repeatability
- Vacuum wavelengths of laser
- Refraction index of the air
- Angle uncertainty (for diffraction methods)
- Interferometer alignment (local probing techniques)
- Sample alignment (local probing techniques)
- Local pitch variations within the central $1mm^2$ (local probing techniques)
- Angular motion of translation stages and Abbe offsets (local probing techniques)

Individual contributions included by some labs which should be considered by others were:

- Influence of mechanical clamping forces (bending)
- Grating temperature deviation from the reference temperature of 20 °C
- Expansion coefficient
- Detector resolution
- Detector calibration
- Various instrument and electronics calibrations
- Interferometer nonlinearity (for local probing techniques)
- Interferometer resolution (for local probing techniques)
- Single line definition (for local probing techniques)
- Sample alignment (for diffraction methods)
- Geometry correction factor, incident angle etc. (for diffraction methods)
- Variation of different diffraction orders (for diffraction methods)
- Variation for different diffraction orientations 0° and 180° (for diffraction methods)

Some laboratories corrected the thermal expansion due to a temperature deviation. Unfortunately the coefficient mentioned in the example of the instructions was the

volumetric and not the linear expansion coefficient. The correct linear expansion coefficient for silicon is about $2.55 \cdot 10^{-6}$ (and not $7.6 \cdot 10^{-6}$).
The consequence of an application of the wrong expansion coefficient is not very dramatic as the contribution for the typical temperature deviations during the measurements of 0.2-0.3°C is very small. A correction for a 1°C temperature deviation with the wrong expansion coefficient of 7.6E-6 would lead in a pitch error of 1.5 pm for the G-300 gratings and 3.5 pm for the G-700 gratings. In the cases of wrong corrections this had no influence for the exclusion from the reference value calculation.

The degrees of freedom were quite differently estimated by the participants, especially for the type B contributions. If the effective degree of freedom of the combined standard uncertainty is rather small but was estimated as infinity, the correct expanded uncertainty could be considerably larger and the corresponding En_{95} value smaller.

11. Discussions, conclusions and remarks

This was the first large international comparison of this type in the field of nanometrology. It took only two years from the decision to carry out this comparison until the first draft report was available. This was possible thanks to the good collaboration of the participants. The number of participants (12) was at the upper limit because of deterioration of the standards during the comparison.
Many different methods and instruments were used and some laboratories applied their method even for the first time. For both gratings the resulting comparison reference value has a very small combined uncertainty of only 1.1 pm and 2.3 pm respectively. As most results are in good agreement with the reference value the comparison was certainly successful. The comparison shows also that all participants are able to estimate reasonable measurement uncertainties. Due to the different methods used, the ratio between the largest and the smallest uncertainty was about 660.
The optical diffraction methods proved to be very successful. Their advantage is that they directly deliver the average pitch over the central measurement surface while the local probing techniques require many sites within this area to be measured and averaged. On the other hand, the SPM methods deliver information about local pitch variations. The performance of the SPM methods in this comparison is also needed to estimate the ability of the participants to calibrate standards with smaller pitches (e.g. < 250 nm) or individual local distances. For the SPM methods the uncertainty is also influenced by local variations of the standards. Better standards with local subnanometre precision would be of advantage.
It can be difficult for optical diffraction methods to judge the quality of a grating especially when there is only one diffraction order available. The uncertainty estimation would be easier for top quality gratings. However, laboratories should be able to deliver a correct uncertainty also for less perfect standards. This is important for calibration services where the quality of the gratings are variable.
PTB has a good value for the 300 nm grating while the measurement on the 700 nm grating has a clear offset. There is the possibility that this measurement was performed when the grating was already damaged. The uncertainty estimation should, however, take the quality of the grating into account.

En values close to 1 (i.e. 1.1) have still a reasonable probability to occur. They were excluded to obtain a reliable reference value. These measurements could be included again if a new detailed estimation of the uncertainty and n_{eff} allows this.
The effect of an exclusion from the comparison reference value calculation is different in each case. For the VNIIM result on the G-700 grating (which is now included for draft B) the influence was less than 0.1 pm because it has only a very small weight. The KRISS result for the G-300 grating has the second smallest uncertainty of all measurements. If included, it has a strong weight and influences the reference value by 1.4 pm. However, this result is not compatible with the others with such a small uncertainty. The inclusion of the PTB result for the G-700 grating would change the reference value by 2.8 pm. This is more than one standard uncertainty of the reference value.

For the optical diffraction measurement methods the uncertainty was in some cases also limited by the quality and rigidity of the standards. The used standards were primarily made for microscope calibrations and not for diffraction. For the diffraction methods only, better suited standards could lead to even smaller uncertainties.
The uncertainties available now at most institutes are sufficient for the calibration of microscope magnification standards. Here relative uncertainties of 10^{-3} are fine. People in this field are also interested in the quality of a grating i.e. the local pitch variations.
As one can see now optical diffraction methods reach uncertainties below 10^{-5}. New applications for such calibrated gratings could become possible: Gratings for monochromators, gratings for laser wavelength comparisons or even gratings for the testing of angular encoder systems.

The traceability to national standards is not yet fulfilled everywhere. Various handbooks were used for the laser wavelengths especially for the non-red ones.
The traceability of the angular measuring devices used for the optical diffraction methods is not always clear or could be improved by using self calibration methods. Three laboratories used other gratings as references and one of these gratings was not traceable to a national standard.
For key comparisons it is required that the participants have an in house traceability for all quantities which give a major contribution to the uncertainty.

Appendix A:

Description of the measurement methods and instruments by the participants

DFM:
DFM has used a commercial atomic force microscope (AFM), a Dimension 3100 system, Digital Instruments, Santa Barbara, USA, with a Dimension Metrology Scanning probe head equipped with capacitive sensors. The nominal maximum scan area is 70µm × 70µm × 6µm. For evaluation of the distances on the recorded images DFM used the PC program SPIP version 1.804, made by ImageMetrology ApS, Denmark. For all uncertainty calculation DFM-GUM, made at Danish Institute of Fundamental Metrology, Denmark, was used.

The calibration of the metrology AFM is based on a two dimensional grid, made by IBSEN Micro Structures A/S, Denmark. The grid has a characteristic lattice spacing in the *x* and *y* direction along with the angle between the two directions. The grating is traceable to NPL (LR0304/99001/DR1/116 - 1999-01-08).

The average pitch was estimated by measuring the pitch distance at 5 different spots as shown in the figure.

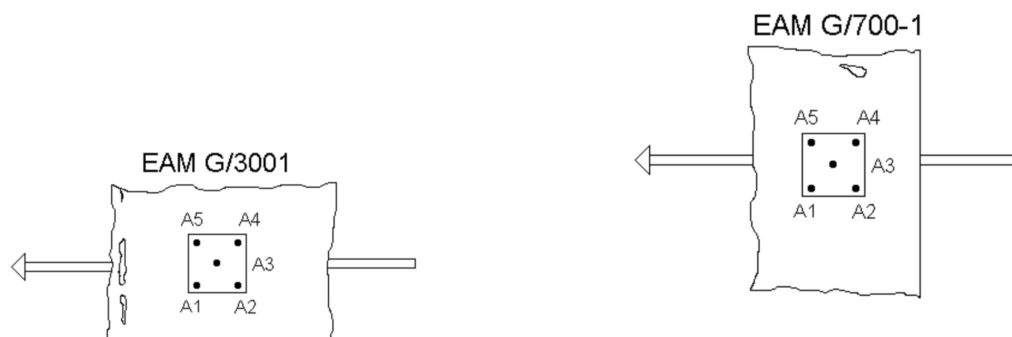

The measurements were performed in the period from 1st of March 1999 to 26th of March 1999. No significant or unexpected damage was observed on the samples.

The measurement procedure follows an A-B-A sequence. First a measurement (A) of the reference is performed, then the unknown line specimen (B) is measured and finally the reference standard (A) is measured again. No drift was observed and no reference measurements were unacceptable.

The temperature was between 19°C to 22°C.

PTB:

The pitch of the gratings was determined by the aid of laser diffraction.
We used a special optical beampath that meets in good approximation the so called Littrow condition. The sample was mounted on a rotating table equipped with a precision angle encoder (Heidenhain RON 255). A CMOS array that was used as detector for the beam diffracted by the sample was placed at a distance of 4 m from the axis of the rotating table and 14 mm below the laser beam which was directed onto the sample without additional optical elements. Although the sample had to be tilted by 0.2 degrees against the axis of the rotating table the influence of the deviation from the exact Littrow condition was negligible as it could be shown by a thorough analysis of the problem. The horizontal angle difference between the two positions of the sample for which beams of corresponding positive and negative diffraction orders met the pixels at the center of the detector was measured. If this difference is $\boldsymbol{Da}$ and the Littrow condition is fulfilled exactly the pitch p of the diffraction structure can be calculated according to the following equation:

$$p = \frac{m\boldsymbol{l}}{2\sin(\Delta\boldsymbol{a}/2)},$$

Where $\boldsymbol{l}$ is the laser wavelength and m the order of diffraction.

The CMOS array consists of 256 diodes with a mutual distance of 50 µm. Their signals were evaluated by means of a computer which presented the signal distribution on the monitor and additionally calculated the position of the signal maximum, i.e. the beam position, within a maximum deviation of one diode distance or an uncertainty of 29 µm, respectively. Thus the detector enabled us to monitor the position of the centers of the diffracted beams with high accuracy.
On each sample twelve measurement cycles at three different wavelength of an Ar-Laser were performed. The repeatability was better than 2 pm for the average pitch of each sample at each wavelength.

IMGC:

The measurement of the two gratings were carried out using a laser diffractometer based on two frequency stabilised lasers (543 and 633nm) and a goniometric table. The measurement consists in measuring the angle between the two positions of the grating corresponding to the autocollimation condition of the two diffracted beams. For the G-300 only the first diffracted order of the 543nm laser is visible, while for the G-700 two diffracted orders are visible both for the 543nm and the 633nm laser leading to four possible measurement conditions.

G-300: A set of about 100 measurements were taken in different times and at different alignment conditions. The main source of uncertainty (as expected) is the error of the goniometric table.

G-700: Four sets of measurements (one for each diffraction condition) were taken, even if the data taken with the second order at 543nm were not used in the analysis because of the weakness of the diffracted beam. In this case all the data where used to calculate the mean value of the pitch but every set of measurement needed a different uncertainty budget. Thus, in the evaluation of the combined uncertainty the contribution of the various errors for the three configurations are reported, but only

the configuration using the first diffracted order of the 633nm laser was used to calculate the final value.

The air refractive index was accurately monitored at regular intervals during the measurement, but a relatively large uncertainty was assigned to this parameter because of possible local temperature and humidity variations due to the open frame structure of the instrument and the presence of the operator.

The effect of the temperature of the gratings was not taken in account, thus the reported results are given for a grating temperature of (20.2 ± 0.2)°C.

NIST:

The average pitch of the specimens EAM G-300/3 and EAM G-700/3 was determined from measurements performed using the NIST calibrated atomic force microscope (C–AFM). The C–AFM is custom-designed AFM for dimensional metrology, and it is intended to calibrate physical standards for other AFMs. The C-AFM has metrology traceability via the 633 nm wavelength of the I_2-stabilized He-Ne laser (a recommended radiation for the realization of the meter in the visible) for all three axes. This is accomplished using heterodyne laser interferometers. The C–AFM employs a scanning-sample design. A piezoelectrically driven two-axis flexure stage, with a 50 µm range, is used to translate the sample in the x and y directions. It has very small straightness and angular motion deviations. Heterodyne laser interferometers monitor the x-y displacement, and a digital signal processor in the controller is used to allow closed loop control of the lateral sample position. This eliminates the scale calibration and linearity problems of the scanners used in most commercial instruments. The vertical (z) position of the sample is adjusted with piezoelectrically-actuated, flexure-guided transducer with an integrated capacitance sensor. This stage provides one axis of rectilinear motion with very small straightness and angular errors, and the capacitance sensor provides measurement of the stage extension with high repeatability and high resolution. To achieve traceability, this sensor must be calibrated using a third interferometer. The system can be operated with several AFM heads, allowing operation in both contact and intermittent-contact modes and the use of both optical-lever force sensors and piezoresistive silicon cantilevers. Low thermal expansion materials and kinematic mounts are used to minimize drifts in the sensitive components of the system, and the instrument is operated in a temperature-controlled laboratory with a stability less than 0.1° C.
Both specimens were characterized using the same basic measurement plan. The central 1 mm^2 portion of the patterned area was measured in nine different locations distributed in a 3 × 3 grid pattern, with approximately uniform spacing (in both directions) of the grid points (i.e. measured locations). At each location, multiple images were averaged to obtain a pitch value for that location. At least three images were used, and for some locations there were more than ten. The location-averaged values of the pitch were then averaged together to obtain the values reported here, and the type A standard uncertainty components were obtained from the standard deviations of the mean (SDOM). We considered 11 influence quantities contributing to the uncertainty of the pitch measurements. These were: repeatability, sample variation, measurand definition (line centering), Abbe errors due to pitch, Abbe errors due to yaw, cosine errors (in plane), cosine errors (out of plane), laser wavelength in vacuum, index of refraction of air, interferometer nonlinearity, and temperature correction. The largest contributions came from the measurand definition and the

Abbe errors arising from pitch. The measurand definition term accounts for the relative uncertainty in choosing the line center from one feature to the next. Hence, the local sample variability also contributes to this term.

NPL1:

Pitch measurement by optical diffraction

A schematic diagram of the equipment used is shown in figure 1. Detail of the mount at the centre of the angle table is shown in figure 2. This mount has adjustments 1 and 2 to enable the active part of the grating to be positioned directly in front of the laser beam. Adjustment 3 is used to ensure the surface of the grating lies along the axis of rotation of the angle table. Adjustment 4 is used to ensure that the diffracted orders lie in the same horizontal plane as the zero order. Adjustment 5 is used to angle the grating surface so that the reflected (zero order) is directed back towards the laser. Once these adjustments have been set, the angle table is rotated so that progressive diffracted orders are directed back towards the laser. Note that the diffracted orders are not sent directly back to the laser, but to a position on the screen which is some millimetres directly above the beam coming from the laser. The laser beam has diameter of approximately 1.5 mm at the grating surface.

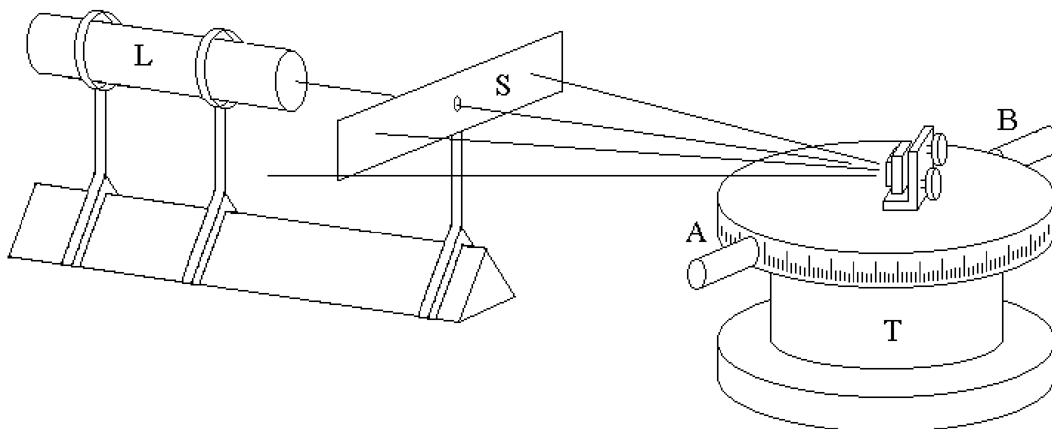

Figure 1. Schematic diagram of the equipment used. Laser L, screen S, angle table T, reading heads A and B

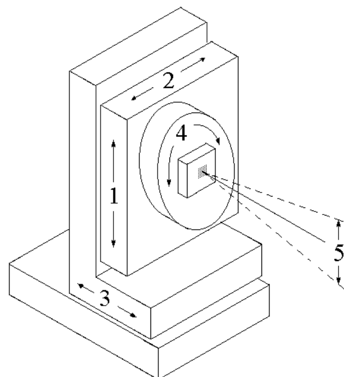

Figure 2. Detail of the central mount on which the grating is located, showing the 5 degrees of freedom used to align the specimen.

Figure 3 shows the condition obtained when the first diffracted order is directed back towards the laser. The angles θ_n at which this condition occurs can be used to calculate the period of the grating using the expression

$$p = \frac{n \cdot \lambda}{2 \cdot \sin \Theta_n} \qquad \ldots(1)$$

Where

p = period n = diffraction order
λ = wavelength θ_n = angle of the *nth* diffracted order.

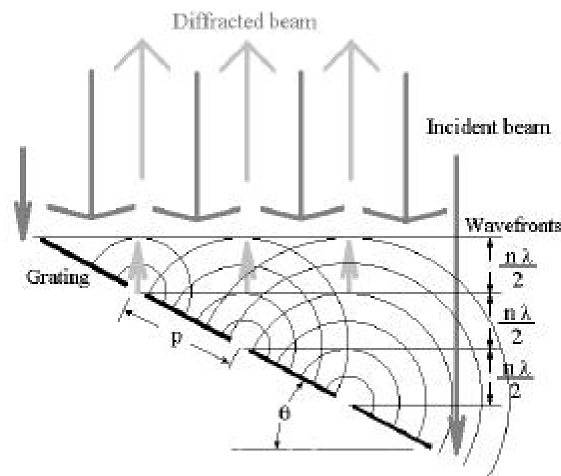

Figure 3: Schematic diagram of the diffraction method used to calibrate the standard.

NPL2:

Optical microscope and Interferometer method

The standards were measured on an optical microscope whose stage is monitored with a helium-neon laser interferometer (see figure 1). A photo-multiplier measures the light transmitted through a narrow slit located in the primary image plane, whilst a piezoelectric transducer moves the stage and the interferometer records the displacement. A computer analyses the data and calculates the distances between features.

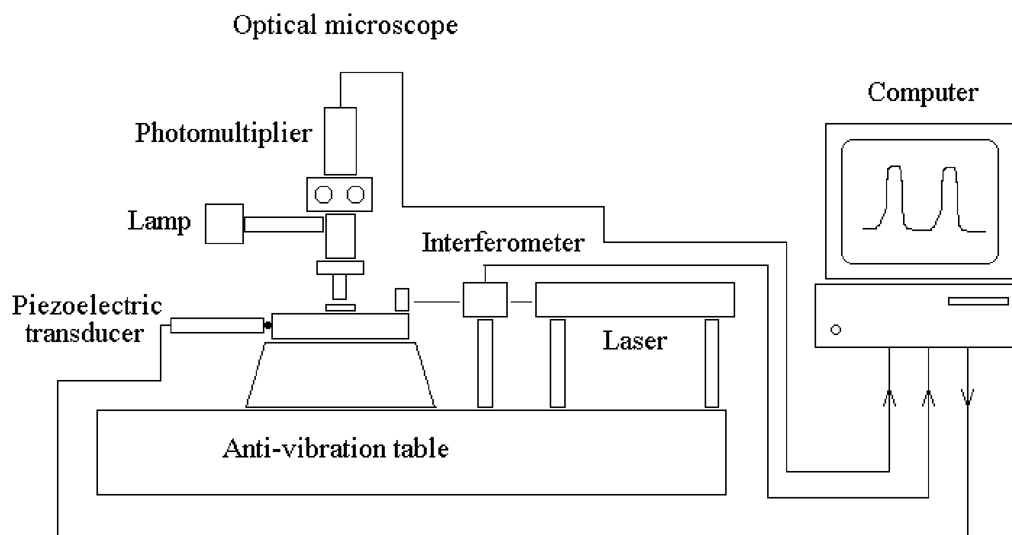

Figure 1. Schematic diagram of the optical microscope used.

Sources of measurement uncertainty:

A - Laser wavelength:
The frequency of the laser was determined by calibration against a reference iodine-stabilised laser and found to be 473 612 504 ± 6 MHz. In practice the uncertainty of approximately 1 part in 10^7 is small compared to the uncertainty due to the refractive index of the air. The worst expected variation in the refractive index of the air is 1 part in 10^6, which is the variation caused by a pressure change of 40 mbar. Using a mean refractive index of 1.0002692 (equivalent to 1000 mbar, 20° C and 50% relative humidity) the atmospheric wavelength of the laser is calculated to be 543.3693 ± 0.0006 nm with a standard uncertainty of approximately 1 part in 10^6 .

B - Angular instability of stage motion.
The yaw and pitch of the stage were measured with an auto-collimator and the standard uncertainty caused by angular instability is estimated to be 6 parts in 10^6 .

C - Interferometer alignment
The cosine error caused by any possible mis-alignment between the stage motion and the axis of the interferometer is estimated to contribute a standard uncertainty of 8 parts in10^6

D - Sample mis-alignment
The cosine error caused by mis-alignment of the sample is estimated to contribute a standard uncertainty of 5 parts in 10^5 .

E - Temperature
The expansion coefficient of common materials used for microscopy standards lies in the range 1 to 16 parts in 10^6 , but over such small dimensions the effects can be neglected. However, the thermal drift in the material making up the microscope and interferometer components can cause appreciable measurement drift. In this optical microscope the measurements are made in both directions (left to right and right to left). The effect of temperature drift is to increase the standard deviation of the measurements, however the mean measurement is unaffected. The effects which tend to increase the measurement spread are taken into account by monitoring the standard deviation of the measurements.

F - Random effects
Other factors considered in the uncertainty calculations include the following:
- Light intensity drifts from the microscope lamp
- Noise on the photo-multiplier signal
- Vibration
- Cyclic errors in the interferometer

All these effects combine to increase the measurement spread and so increase the standard deviation. The standard uncertainty is thus calculated from each measurement run which includes 5 positive going and 5 negative going measurements. The magnitude will depend on the environmental conditions prevailing at the time of measurement. The standard uncertainty is calculated and combined with all the type B uncertainties.

Measurement results:

Only EAMG-700/3 could be measured with the optical microscope because EAMG-300/3 was too small for optical resolution.

The length of cumulative periods of the grating were measured at 12 random sites spread over the surface of the grating. The scan length was approximately 175 micrometers and included approximately 250 consecutive pitches. The measured pitch given in the table below is the average of the measurements at the 12 sites. The uncertainty budget is that associated with the measurement at one site. Figure 2 shows the pitch variations measured across the 12 sites.

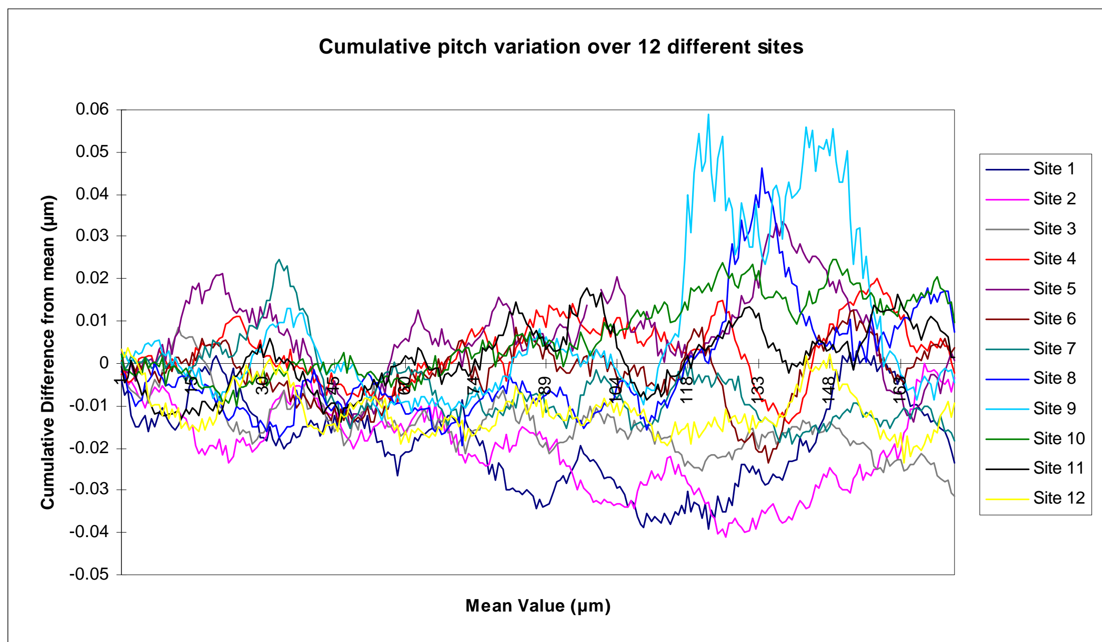

Figure 2. Cumulative pitch variations over 12 different sites.

VNIIM:

The measurements of the average pitch (spacing) were carried out by the interference diffractometry method (see: V.I. Korotkov, S.A. Pulkin, A.L. Vitushkin, L.F. Vitushkin Appl.Optics, 1996, vol.36, No 24, pp.4782-4786). The spacing (average pitch) (P) is evaluated from the ratio of the measured periods (p_0/p_1) of the interference fringes defined by the angles between the beams diffracted from the reference grating (line scale) and from the grating to be measured. The setup – laser interference diffractometer (LID) has been used for the measurements. The optical scheme of LID is the optical scheme of the Michelson interferometer with optical system for obtaining the interference pattern on the CCD – camera (1 dimensional). The reference line scale and investigating grating were placed to the arms of the interferometer . The alternative absolute 3-wavelength method (without reference line scale) was used too. The coincidence of the results between these two methods was some additional criterion for correctness of the measurements.

The uncertainty of measurements has been estimated according to ISO Guide to the Expression of Uncertainty in Measurement:

1. The measurand P is given by the functional relationship :

   $P = (\lambda_0^2/4 + (1/\gamma^2)((\lambda_0/2)(1+(1-\gamma^2)^{1/2}) - \lambda_1)^{1/2}$,

   Where $\gamma = (p_0/p_1)\lambda_1/2d_0$.

   Then P is the function of 5 input quantities :

   $P = f (p_0,p_1,d_0,\lambda_0,\lambda_1)$, where

   p_0 – is the period of interference fringes, when the (+) 1-order beam interfere with (-)1- order beam of diffraction from reference standard (line scale)

   p_1 – is the period of interference fringes, when the 1-st order beam of diffraction from investigating grating interfere with 0-th order beam from reference standard on wavelength λ_1.

   For the wavelength λ_0 the autocollimation condition is satisfied :

   $2 P \sin \varphi = \lambda_0$.

   For the wavelength λ_1 one can see :

   $P (\sin \varphi + \sin \alpha) = \lambda_1$.

   The ratio of periods of interference fringes is determined as:

   $p_0/p_1 = \sin \Phi_1/\sin 2\Phi_0$, where the angle Φ_0 is determined from the known period of reference standard: $d_0 \sin \Phi_0 = \lambda_0$. The angle $\Phi = \alpha-\varphi$.

2. The evaluation of uncertainty.

2.1.Type A evaluation of standard uncertainty was made from the experimental statistical data of measurements of periods of interference fringes p_1 and p_0 .
The average periods p_i and its experimental standard deviations are obtained from the results of computer treatment of the interference pattern signal on the CCD – camera after averaging of the pitch on the range ~ 1 mm on the central part of the grating surface. It is not necessary to calibrate the CCD – camera absolutely because only ratio of periods is included in the working formula. Then only the relative units for periods are possible to use.

2.2. Type B evaluation of standard uncertainty was made from the estimation of possible influence parameters.

2.2.1. The calibration of the reference standard (line scale) with period $d_0 \approx 5.00$ µm was carried out on the National Length Standard with standard uncertainty given in certificate of calibration $u(d_0) = \theta(d_0)/\sqrt{3} = 0.02/\sqrt{3} = 0.0115$ (µm).

2.2.2. The angle uncertainty is determined by the uncertainty of alignment of the infinity wide fringe. The alignment of the infinity wide fringe is made on the wavelength λ_0 visually. For autocollimation angle φ the estimation of bounds $\theta(\varphi)$ can be calculated from the condition, when the width of fringe is equal to illuminated region of grating s : $s * \sin \theta(\varphi) = \lambda_0$. For s = 3 mm - $\theta(\varphi) = 1.7 * 10^{-4}$ rad. This disalignment leads to changing of the diffraction angle α and to the period of interference fringes p_1(determined by the interference angle Φ): $\sin(\alpha + \theta(\alpha)) = \lambda_1/P - \sin(\varphi +\theta(\varphi))$ and $\Phi +\theta(\Phi) = (\alpha + \theta(\alpha))) - (\varphi + \theta (\varphi))$. The standard uncertainty $u (\Phi) = (\partial f/\partial\Phi)u(\Phi) = (\partial f/\partial p_1)(\partial p_1/\partial\Phi)u(\Phi)$,where $\partial p_1/\partial\Phi = \lambda_1 \cos \Phi / \sin^2 \Phi$. Calculations give us the bounds for interference angles $\theta(\Phi) = 3.78 * 10^{-4}$ rad (for G-300) and

$\theta(\Phi)$ = 3.99 * 10^{-4} rad (for G-700) . The standard uncertainty is determined from bound : $u(\Phi) = \theta(\Phi)/\sqrt{3}$.

2.2.3. The wavelength uncertainty was estimated from the bounds for measured argon laser wavelengths given in “Handbook of lasers with selected data on optical technology” (Edited by R.J. Pressley. Chemical Rubber Co, Cleveland, 1971):

λ_0 = 0.501717 µm $\theta = 2*10^{-6}$ µm
λ_1 = 0.514532 µm $\theta = 2*10^{-6}$ µm
λ_2 = 0.487986 µm $\theta = 4*10^{-6}$ µm

2.2.4. The measurements were made on the reference temperature of 20 ºC with standard uncertainty u(t) = 0.3º and measured pitch is given for the reference temperature.

3.The list of the parameters for calculation of the pitch:

λ_0 = 0.501717 nm
λ_1 = 0.514532 nm
λ_2 = 0.487986 nm
d_0 = 5.00 µm

for G-300	for G-700
p_0 = 17.328	p_0 = 17.341
p_1 = 17.759	p_1 = 33.017
p_2 = 18.675	

Note: λ_2 and p_2 were used in treatment by 3-wave absolute method (without reference standard).
The result of the measurements by this method coincides with 2-wave method, but uncertainty is large, as one can see from Table (G-300-3wave), therefore in Table “Measurement results” we did not use the 3-wave method results.

NIM:

The measurement instrument based on diffraction method is shown as the figure 1, which is called Littrow diffraction system. The grating is installed on digital rotating table of the responsive synchronous instrument (The angular uncertainty in arbitrary position is U_{95} = 1.939·10^{-5}(rad)). When the laser of 543 nm or 633 nm is illuminated on the grating surface, firstly make zero grade of diffraction shine on two quadrants photoelectrical receiver, whose output is the difference signal of two quadrants.

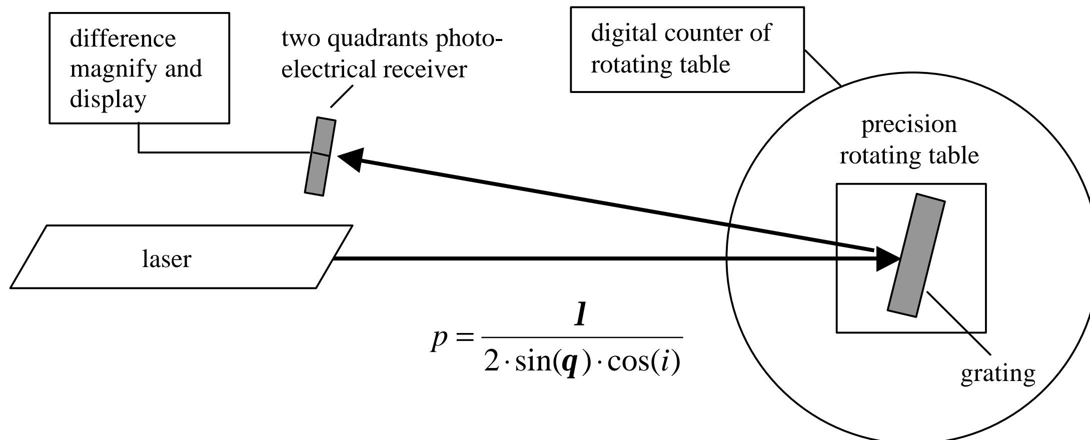

Figure 1. The theory picture of measuring system

When the signal is zero, clear the value of rotating table. And then turn the table so as to make + 1 and – 1 grade of diffraction fall in photoelectrical receiver in turn. Record the value of rotating table, that is the corresponding diffraction angle, while the output signal of the receiver is zero. The purpose of measuring + 1 and – 1 grade of diffraction at the same time is to eliminate unsymmetric influence of optical system, diffraction light spot and photoelectrical receiver. Each standard is measured ten times independently. After getting the diffraction angle, we can calculate the pitch of grating on the basis of the following formula:

Where: λ - the wavelength of laser at 20°C,
θ - the diffraction angle, i – the incidence angle.

The temperature is room temperature. The beam spot size on the grating is about 2.5 mm. The direction of angular difference between the incoming laser beam and the beam going to the detector is horizontal which is described as the incident angle i and has been measured. The angle in vertical direction is less than 1', that less influenced the measurement value. Therefore it is neglected. The angles in horizontal direction were 0.001459 rad for EAM G-300/3 with green laser, 0.001589 rad for EAM G-700/3 with green laser and 0.001911 rad for EAM G-700/3 with red laser.

NRLM:

An interferometrically measuring atomic force microscope was used for this comparison. Maximum scan area is 17.5(X) x 17.5(Y) x 2.5(Z) µm. Detailed discriptions of measurements and analyses are described below.

1. Measurements
   The profiles were taken with a contact mode (force constant mode) of AFM. Conical, rectangular-shaped cantilevers were used in this measurement. The nominal spring constant is 0.05 N/m. 10-12 local areas were selected within a 1 mm square of the center of the sample. At each local area, three measurements were repeatedly performed. A measurement includes the 14-20 scans with the direction orthogonal to lib of the gratings. Scanned data were acquired with a three-axis laser interferometer as three-dimensional position data array along the scanning path of a stage. The measurement parameters are listed below.

Sample	Scan length / line	No. of data point / line	No. of pitch / line (typical)	No. of scan lines / measurement	No. of measurements / local area	No. of local areas / sample
EAM G-300	10.0 µm	5,500	36	20	3	10
EAM G-700	17.5 µm	8,000	26	14	3	12

2. Analysis

   The pitch values were obtained through following steps.

   (1) Laser wavelength ....
   The wavelength of the lasers at every measurements was calibrated using Edlen's equation with the values of ambient temperature, air pressure, and humidity. Sensors for these parameters were calibrated by NRLM's other sections. The uncertainties of calculating a correction factor is negligible. The frequency of the lasers used in this measurements was calibrated in comparison with that of an I_2-stabilized He-Ne laser. The frequency stability was evaluated from the Allan variance of the beat frequency of a target laser and i component of the I_2-stabilized laser.

   (2) Slope correction ....
   The center line of the undulation of profiles was obtained from the least square fitting using the peak and valley points. Leveling and slope correction were carried out with the slope of the center lines.

   (3) Calculation of peak position ....
   At first, the zero-crossing points at both sides of each peak on the base line were calculated. Next, the center of gravity of the area bounded by a peak and the base line was obtained. At last, the X position the center of gravity is taken as the representative value of the peak position.

   (4) Pitch calculation and correction of the cosine error..
   The average pitch was calculated using all the peak positions from 14 or 20

lines containing 720 or 364 peaks, respectively. Cosine errors occur when the direction of the scan is not perfectly perpendicular to the lib of the grating. The correction, therefore, was conducted using the tilt angle calculated from peak points lying on an identical peak.

(5) Correction for the thermal expansion ....
The average temperature of sample during measurement was 22.5°C. The resulting values were corrected to values corresponding to 20°C. 2.6 E-6 K^{-1} was chosen as a coefficient of thermal expansion. This value refers to that of other section of NRLM for a silicon single crystal. Several values found in other literatures vary from 2.6E-6 to 7.6E-6 K^{-1}.

CMS:
Our Grating Measuring System is an Atomic Force Microscope, which is manufactured by **di** (Digital Instruments). The model type is Dimension 3100M.
Our reference grating standards is manufactured by Moxtek. The model type is MXS 301BE. The Moxtek calibration certificate gives a calibrated pitch of 292 nm with an accuracy (3 sigma) of ± 1%.
For the specimens and standards, the measurements are taken at 9 sites over the central surface area of 0.5 mm × 0.5 mm as shown in Figure 1. For each site, we measured 3 times. Thus, there are totally 27 measurements for each specimen and standards.

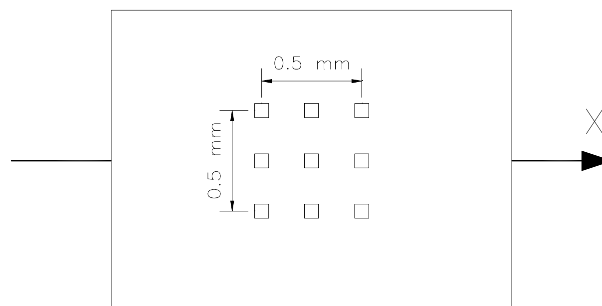

Figure 1 Central measurement surface 0.5 mm ´ 0.5 mm

For specimens with nominal pitches of 290 nm, the scan size of each site is 3 µm × 3 µm. For the specimen with nominal pitch of 700 nm, the scan size of each site is 7 µm × 7 µm.
The images are then analysed to calculate the pitches by using an software called Scanning Probe Image Processor (SPIP), which is established by Image Metrology (http://www.imagemet.com). Thus, the pitches of the specimens can be compared with that of our reference standards.

KRISS:
The mean pitch over the center area of the specimens were measured by the diffraction method (Littrow mounting). The converging laser beam was incident on the center of the specimen at which the spot size is approximately 0.7 mm (normal incidence). The diffraction angle (anti-reflecting angle) was chosen as the angle readout of the sample stage as the diffraction spot is located on the center of the quad. The first-order (for EAM G-300/3) and second-order (for EAM G-700/3) diffraction angles were used to obtain the mean pitch through grating formula. As a

diffraction angles, average of two diffraction angles at both sides was chosen. The measurements were repeated 10 or 6 times while relocating the laser spot on the center area at each time. Such a repetition was performed in three independent setups, and the total 22 data were obtained for each specimen. As a light source, argon ion laser (λ=487.986 ± 0.004 nm) was used. The uncertainty of the wavelength was quoted from a reference*. The rotary table with the angle encoder (resolution 0.0001°) coupled inside was used to rotate the specimen. The angle-readout was calibrated with the indexing table (accuracy 0.1”), and found to be accurate within 0.0004°. The temperature of the specimen was measured with the contact-type thermometer (error not greater than 0.02 °C) mounted on a surface of the holding block of the grating specimen. The temperature was taken at each measurement of a diffraction angle. The obtained pitch were corrected considering thermal expansion coefficient of the silicon substrate. The refractive index were calculated with the Edlen formula from the measured air temperature, relative humidity, air pressure and CO_2 concentration near the light path. The effect due to the deviation of diffracted beam out of the incidence is estimated so small that it was not considered in the uncertainty analysis.

*Marvin J. Weber, *Handbook of Laser Wavelengths*, (CRC Press Boca Raton Boston London New York Washington, D.C. 1999) p.308.

OFMET1:
Pitch measurement by optical diffraction

A detailed description of the experimental set-up can be found in the proceedings of the euspen conference, Bremen May 1999, Vol. 2, p. 525-255.

The diffractometer as shown in figure 1 is placed on a granite table. The laser beam passes a beam splitter and falls onto the grating under test where the light is

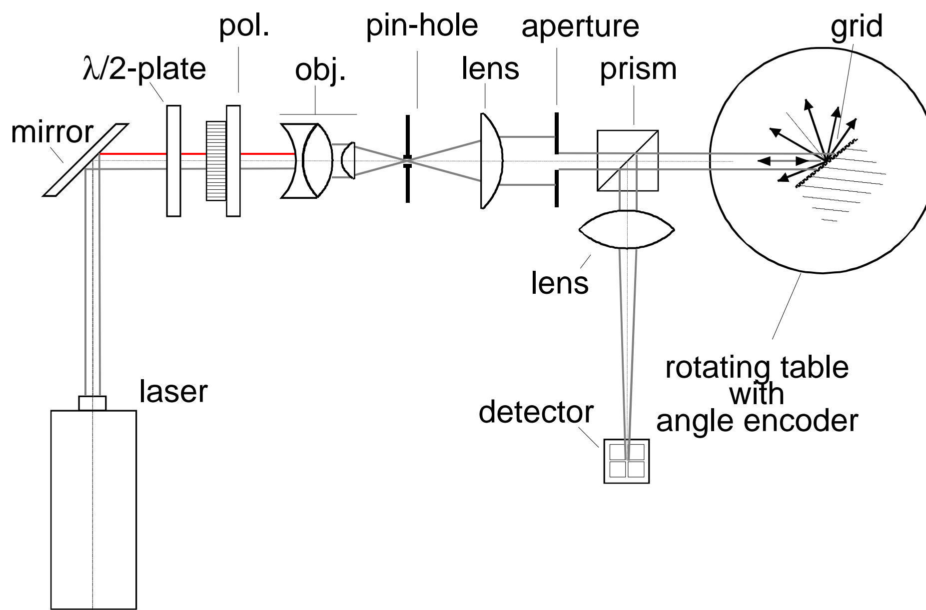

Figure 1: Experimental arrangement of the laser diffractometer (top view).

diffracted. As the laser beam is spatially filtered is has a gaussian intensity profile and an improved beam pointing stability. At certain angles the diffracted angle coincides with the incident angle (Littrow diffraction). At this condition the light is

reflected back through the beam splitter and a focusing lens onto a 4-quadrant photo-detector. The photo-detector is also used vertically to adjust the in-plane orientation of the grating to minimise the cosine error.

For Littrow diffraction the pitch is calculated as follows:

$$p = \frac{m \cdot \lambda}{2 \cdot \sin \beta}$$

p = pitch, λ = laser wavelength, m = diffraction order, β = diffraction angle

The rotary table has air bearings and an incremental encoder for the angular measurements (Heidenhain, RON 905). The resolution is 0.035 arcsec and the accuracy 0.07 arcsec for any angular position. The rotary table is driven with a dc-motor and a friction wheel. The fine adjustment is made with a piezo driven lever. It is our national standard for angles. Traceability comes from self calibration methods with optical polygons and a Moore indexing table, verified through international comparisons.
The lasers used were an unstabilised red He-Ne laser and a green mode stabilised He-Ne laser. The centre frequency of the gain curve of the red He-Ne laser was calibrated with a I_2-stabilised laser resulting in a relative standard uncertainty of $u_c = 6.4 \cdot 10^{-7}$. The green He-Ne laser was calibrated by a comparison with the red laser through several diffraction measurements on a 700 nm grating resulting in a relative standard uncertainty of $u_c = 3.2 \cdot 10^{-6}$. Pressure and temperature were monitored to calculate the refraction index of the air by the Edlen formula.
The temperature of the air around the sample was measured and the thermal expansion was corrected to values corresponding to 20°C with α =2.6 E-6 K^{-1} and ΔT typically 0.5°C ± 0.4°C.
A short measurement time reduces the influence of drift. Once the initial adjustments are made, the measurement of all diffraction lines takes only about 2 minutes.
There are 9 influence quantities considered for the uncertainty of the measured pitch: Angle uncertainty, repeatability of the angular detection, variations between different diffraction orders, variations between different grating orientations (up, down), variations due to different clamping, laser wavelength, refractive index of the air, cosine error and temperature deviation. The largest contribution to the total uncertainty was due to the variations between the different diffraction orders and variations due to different clamping observed on gratings of the same type in the course of preliminary studies. For the G-300 gratings, where only one diffraction order can be observed, the observed variations on the G-700 gratings were used as estimates of these influences.

OFMET2:
AFM profiler with interferometer
A detailed description of the experimental set-up can be found in Measurement Science and Technology, **9**, 1998, p. 1087-1092.
The AFM profiler system combines a linear long range sample displacement stage with a commercial metrology AFM (Dimension 3500 with metrology head from Digital Instruments). The linear displacement stage provides a very straight motion over a range of 380 µm. The displacement is measured by a subnanometer resolution interferometer at nominally zero Abbe offset (Fig. 1).

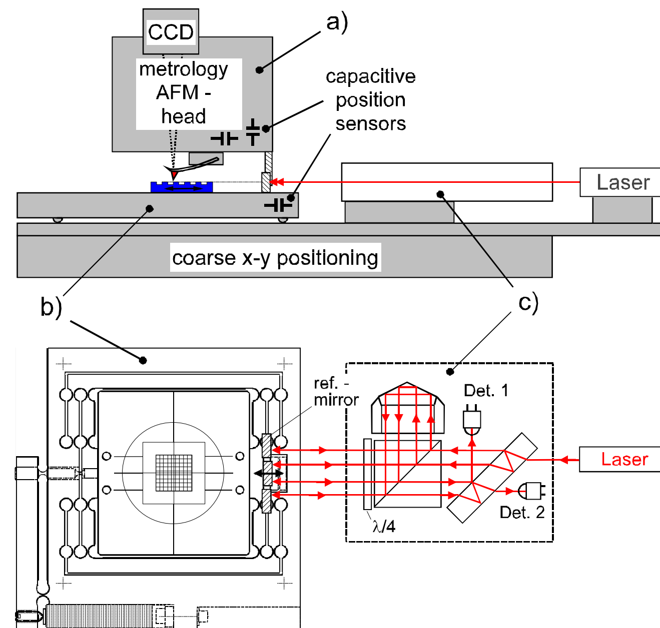

Fig. 1. General setup of the long range AFM profiler system. a) metrology AFM head including a video microscope, b) piezo actuated linear long range displacement stage with monolithic flexures forming a double parallelogram and c) schematic of the differential double pass plane mirror interferometer with HeNe-laser.

An optical zoom video microscope and a coarse x-y table allow an easy positioning of the location of interest below the tip. The linear long range displacement stage consists of monolithic flexures forming a double parallelogram. The stage is actuated by a piezo whereby a lever amplifies the motion by a factor of 6 to provide a displacement over 380 µm. Pitch and yaw of the motion were measured with an autocollimator. They are almost linearly increasing with the displacement to 0.6 and 0.7 arcsec over the full range. An Abbe offset < 1 mm gives therefore an error of less than 3 nm over 380 µm.
The position of the linear displacement stage is adjusted by a feedback using a capacitive position sensor (Queensgate) while the position measurement is made with a double pass differential plane mirror interferometer (NPL). To obtain a linear phase interpolation a numerical method described by Heydemann is applied.
The measurement strategy used was the following: The linear stage produced offsets which were multiples of the pitch. At each stage position the AFM head was used to locate the line centre with the centre of gravity method evaluating 1000 points over one pitch. The AFM was always operated in tapping mode. The position of five to ten features was measured several times over a range of 288 µm (G-300) and 350 µm (G-700). The average pitch of a profile was calculated from the slope of

a linear fit to these measured locations. To reduce the effect of drift always a pair of up and down profiles were evaluated. Profiles in five different locations within the central 1 mm x 1 mm were measured on each of the gratings.
The uncertainty budget contains 12 influence quantities: Laser wavelength, refractive index of the air, interferometer nonlinearity, interferometer alignment, sample alignment lateral and horizontal, yaw and pitch of the motion with Abbe offset, temperature deviation, AFM calibration, the repeatability of the measurement in one place and the spread in the different locations.
The largest contribution to the total uncertainty was for both standards the local pitch variation.